

NPS ARCHIVE
1968
FANTIN, J.

AN INVESTIGATION OF THE CHARACTERISTICS
OF SWIRLING FLOW IN A DIVERGING TUBE

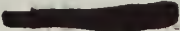
JON RONALD FANTIN

DUDMAN LIBRARY
NAB GRADUATE SCHOOL
MONTANA CA 93943-101

AN INVESTIGATION OF THE CHARACTERISTICS OF
SWIRLING FLOW IN A DIVERGING TUBE

by

Jon Ronald Fantin
Lieutenant, United States Navy
B.S., California State College at Los Angeles, 1962



Submitted in partial fulfillment of the
requirements for the degree of
MASTER OF SCIENCE IN MECHANICAL ENGINEERING

from the

NAVAL POSTGRADUATE SCHOOL
June 1968

1P Archive
1968
Forthin J.

Therob
F2X3
Q.1

ABSTRACT

The effect of an imposed pressure gradient on the core of a vortex is examined both theoretically and experimentally. The test apparatus consisted of a vortex chamber and a diverging tube. The swirling flow was generated by means of adjustable vanes at the periphery of the vortex chamber and by introducing varying amounts of air. Pressure distributions were obtained along the wall of the tube for various flows and vane settings. In addition, the core of the vortex was photographed by introducing smoke at the axis of the vortex chamber.

The theoretical and experimental results show the existence of standing waves arising from the vortex breakdown and the existence of critical conditions, depending on the ratio of the rotational and longitudinal velocity components, beyond which drastic changes of flow structure must occur. The theoretical results were found to be closely related to the observed phenomena.

TABLE OF CONTENTS

Section	Page
1. Introduction	13
2. Experimental Equipment and Procedure	18
3. Theoretical Considerations	22
4. Discussion of Theoretical and Experimental Results	25
5. Conclusions	28
6. Recommendations for Future Work	29
Bibliography	30
Figures	31
Tables	47

LIST OF TABLES

Table		Page
1.	Experimental data for the calculation of circulation for the vane setting of 36.5 degrees	47
2.	Experimental data for the calculation of circulation for the vane setting of 45 degrees	47
3.	Experimental data for the calculation of circulation for the vane setting of 60 degrees	48
4.	Experimental data for the calculation of circulation for the vane setting of 70 degrees	48

LIST OF FIGURES

Figure		Page
1.	The Two Forms of Vortex Breakdown	31
2.	Schematic of Vortex Chamber and Divergent Tube	32
3.	Arrangement of Experimental Equipment	33
4.	Sketch of Vane Orientation	34
5.	Photograph of Vane Section and Chamber Inlets	35
6.	Mathematical Model of the Vortex Core	36
7.	Normalized Graph of Axial Velocity vs. Tangential Velocity	37
8.	Static Pressure Distribution Along Tube (Vane Setting 36.5°)	38
9.	Static Pressure Distribution Along Tube (Vane Setting 45°)	39
10.	Static Pressure Distribution Along Tube (Vane Setting 60°)	40
11.	Static Pressure Distribution Along Tube (Vane Setting 70°)	41
12-16.	Examples of Visualization of Vortex Breakdown	42-46

NOMENCLATURE

b	thickness of vanes
C_p	pressure coefficient $\frac{\Delta P}{\frac{1}{2}\rho U_1^2}$
D	outside diameter of vortex chamber
d_1	inside diameter of the uniform portion of the tube
d_2	inside diameter of tube at downstream end
J_0	Bessel function of zero order
J_1	Bessel function of first order
L_1	length of vortex chamber
L_2	length of the divergent tube extending from vortex chamber
P_1	static pressure at section C_1 (See Fig. 6)
P_2	static pressure at section C_2
Q	flow rate
R_1	radius of core at section C_1
R_2	radius of core at section C_2
r_1	inside radius of the uniform portion of the tube
t	perpendicular distance between vanes
U_1	uniform longitudinal velocity at C_1
U_2	uniform longitudinal velocity outside core at C_2
u	$\frac{u_2}{U_2}$
u_2	longitudinal velocity component in core at C_2
V	rotational velocity component at the edge of the core
V_r	radial velocity in vortex chamber
V_t	tangential velocity in vortex chamber
V'	total velocity in vortex chamber

v_1	rotational velocity component in core at C_1
v_2	rotational velocity component in core at C_2
x	axial distance from upstream end of tube
z	distance from axis of vortex chamber to vanes
α	$2 \frac{VR_2}{U_1 R_1}$
β	$\frac{U_1}{U_2}$
Γ	circulation
δ	probe angle
η	$\frac{\eta_2}{R_2}$
η_1	radius within core at C_1
η_2	radius within core at C_2
θ	vane angle
ρ	density

ACKNOWLEDGEMENT

The work described herein was made possible through the sponsorship of the Harry Diamond Laboratories of the United States Army Material Command, Washington, D. C. The author wishes to express his appreciation to Professor T. Sarpkaya for his guidance and encouragement during the course of the investigation. A special note of appreciation is also given to Messrs. K. Mothersell, J. Beck and J. McKay, of the Mechanical Engineering Machine Shop, for their efforts in the constructing of the experimental equipment.

1. Introduction.

During recent years, interest has been generated in a flow phenomenon that has become known as the vortex breakdown, or vortex bursting. Vortex breakdown is the abrupt structural change that occurs in a swirling flow at some definite axial position. It has been observed in the swirling flow generated on the upper surface of a lifting delta wing, or one with high sweep back, when the angle of attack is sufficient to cause separation at the leading edge. The phenomenon has also been observed in the confined swirling flows of vortex whistles (1) and cyclone separators (2).

Depending on whether the vortex flow occurs over wings or is confined in tubes, different types of breakdown have been observed. Two extreme forms can be recognized as shown in Figure 1. These forms are clearly differentiated by the behavior of the axial core of the vortex, as pointed out by Lambourne and Bryer (3). In the steady, axisymmetric form, the axial core expands to become a surface enclosing a bubble. In the periodic, spiral form, the axial core remains, but it is deformed into a spiral. In both forms, the flow becomes turbulent further downstream.

A large number of theoretical and experimental studies on leading edge vortices, on confined steady flows in general, and on swirling flows with temporal and spatial periodicity in particular have been initiated. These studies were stimulated by the development of high-speed aircraft with slender wings whose leading edges are highly swept back, the development of nuclear rocket propulsion using gaseous core reactors, electric power generation using magneto-hydrodynamic effects, vortex valves, and pure fluid pressure modulators for pneumatic amplifier systems.

Since vortex breakdown was first discovered by Peckham (4) in 1957, a number of explanations of its nature have been proposed. The following discussion describes some proposed explanations and investigations of the phenomenon.

Squire (5) presented a theoretical study, based on small perturbations analysis, suggesting that breakdown occurs when the flow can sustain infinitesimal standing waves. If such waves exist, disturbances which are present downstream will spread along the vortex and disrupt the flow near the start. Since standing waves of indefinitely great length are the ones to first become possible as the velocity increases, Squire proposed the limiting condition for the existence of such waves to be the inception state for vortex breakdown. He concluded that, for a constant axial velocity and given distribution of swirl velocity, the ratio of the maximum tangential velocity to that in the axial direction (the tangent of the maximum swirl angle) is the only characteristic parameter determining whether the breakdown will occur, and that this critical value will be in the range of 1.0 to 1.2.

Harvey (6) conducted a series of experiments, using a vortex tube, and showed that for low swirl settings a classical vortex is obtained. As the setting of vanes is changed to give a larger swirl, vortex breakdown, in the form of a spherical bubble of a stagnant fluid, is precipitated. He observed that the flow does not immediately break into an unsteady, random motion, but instead retains a well organized character to the extent that normal vortex flow is once again restored downstream. Finally, for high swirl settings, breakdown disappears, leaving a second type of vortex flow -- one with a core region in which the general flow direction is reversed. From his observations, Harvey concluded that the

breakdown is a phenomenon bridging the gap between two states of conjugate rotating flows.

The comprehensive work of Chanaud (7) on temporal periodic motion in a vortex whistle and cyclone separator suggests that both the flow reversal and amplifications of small disturbances contribute to the hydrodynamic instability of confined, swirling flows. This suggestion is, as pointed out by Chanaud, in conformity with that made earlier by Gartshore (8) on theoretical grounds.

Benjamin (9,10), departing radically from previous theories, provided a formulation for the anticipated vortex breakdown by considering the phenomenon to be an abrupt and circulation-preserving transition of finite magnitude between two dynamically conjugate states of axially symmetric, steady, inviscid flow. Benjamin attempted to prove that breakdown marks not the onset of instability, but rather a finite transition between two conjugate states of flow. He stated that a mild vortex breakdown - one for which the difference between two conjugate states is small - manifests a periodic structure analogous to a weak wave like hydraulic jump, whereas a strong breakdown requires considerable dissipation of energy, as in the turbulent front of a strong hydraulic jump.

Hall(11) has presented an exploratory numerical approach to vortex breakdown by use of a finite-difference technique. He proposed a mathematical model of the vortex core, with the shape of the confining tube and the initial upstream conditions prescribed. Hall's investigation was confined to flows which were quasi-cylindrical. These assumptions permitted the calculation of velocity and pressure distribution for the prescribed boundary conditions. Hall's objective was to see if the

theoretical flow undergoes any abrupt change under conditions approximating those encountered in practice when vortex breakdown occurs. He concluded that vortex breakdown seemed not to be related to instability and that a sudden slowing of the fluid occurred near the point of breakdown. But he also pointed out that abrupt changes might result from the inadequacies of the mathematical model rather than from the physical situation.

Because of the uncertainties resulting from the investigations described above, further investigation of vortex breakdown, with a vortex less complicated than that produced by a swept leading edge, had to be considered. For this reason, the vortex chamber-divergent tube combination shown in Figure 2 was constructed, and the resulting swirling flow was investigated.

There are, to be sure, considerable structural differences between a confined tube vortex and a leading edge vortex, as indicated by Lambourne and Bryer (3). In generating a tube vortex, angular momentum about the longitudinal axis of the tube is imparted to the fluid during its passage between vanes. It might be expected that, since each ring of fluid around the axis of the tube has received the same angular momentum, the vortex would have the structure of a potential vortex with infinite vorticity along the axis. However, because of viscous effects, a vortex in a tube has a core. The core is continuously fed by the boundary layers occurring on the chamber walls. Unlike the leading edge vortex, with its continual feeding of vorticity to the vortex core, the tube vortex has no increase of strength along its length.

Differing from the previous confined-vortex investigations, the cross-section of the vortex tube was uniformly increased for the purpose of

eliminating the constricting effects of the boundary layers of the tube wall and for the purpose of controlling the location of the breakdown. The previous investigations have shown that the location of the vortex breakdown is determined by the conditions prevailing in the downstream section of the tube, in the same way that location of a hydraulic jump on a supercritical stream in an open channel is determined by the backwater conditions. Moreover, just as some sort of obstruction in the channel is necessary to precipitate a hydraulic jump on a supercritical stream, the vortex breakdown requires one or more triggering agencies such as the countervortex in Sarpkaya's studies (12), or an adverse pressure gradient created by the divergence of the vortex tube.

The objectives of the present investigation were to study the effect of the adverse pressure gradient on the inception and location of the vortex breakdown and to show the existence of wavy flows arising from vortex breakdown. For this purpose, pressure distributions were obtained along the vortex tube and it has been shown conclusively that the first wave of a mild vortex breakdown is followed by other waves until the flow becomes fully turbulent. The existence of such waves strongly suggests their inherent role as the basic state upon which the actual flow subsists, developing as a result of instability or of incidentally imposed fluctuations.

2. Experimental Equipment and Procedure.

The experimental equipment consisted of a vortex chamber, divergent tube, rotameter, pressure regulators, pitot tube, pressure transducer and an amplifier-recorder assembly. Figure 3 shows the arrangement of the equipment. The vortex chamber and divergent tube are shown schematically in Figure 2.

The vortex chamber consisted mainly of four parts, all of which were made of plexiglass. The four parts are the cap, chamber body, vanes, and the coupling ring. The cap was removable, and was streamlined towards its center. A hole was provided in the cap to allow a 1/16 inch diameter pitot tube to be inserted into the vortex chamber. The cap was also furnished with a hole in its axis. The hole was used to introduce smoke into the swirling flow for visualization purposes.

The chamber body was streamlined in a manner similar to that of the cap, to provide a uniform cross section at any radius. The downstream face of the chamber body contained a threaded hole by which the divergent tube could be attached to it. The upstream face of the chamber body was fitted with equally spaced holes around its periphery. The holes were used for mounting the vanes and also provided a means of rotating the vanes to various angles. Both the cap and the body were mirror polished, especially the streamlined surfaces.

The vortex chamber contained fifteen equally spaced, variable incidence vanes. The vanes were used to impart a swirl to the flow. The vanes were set successively at 36.5° , 45° , 60° , and 70° in the experiment, the angles being measured as shown in Figures 4 and 5. The vanes were 0.466 inches thick and were bolted to the chamber body.

The coupling ring which surrounded the cap and chamber body contained six equally spaced plexiglass hose connections which were used as inlets to the vortex chamber. The space between the chamber body and the coupling ring was filled with layers of foam rubber. The purpose of the porous material was to reduce perturbations in the flow and to establish a more uniform velocity distribution around the periphery of the chamber.

The twelve inch long divergent tube was made of plexiglass and was carefully polished on both its inner and outer surfaces. The outside diameter of the tube was 2.00 inches. The inside diameter consisted of a uniform section and a diverging section. The uniform portion was 1.00 inch in diameter and was 2.00 inches long. The remaining section started at 1.00 inch and diverged to 1.50 inches in diameter at the end of the tube. The tube contained eighteen wall pressure taps, all at the same radial position. The taps were 0.021 inches in diameter and 0.50 inches apart in an axial direction. When the vortex chamber and tube were assembled, care was taken to provide a smooth transition between the chamber body and the inside diameter of the tube. The downstream end of the tube was left open to the atmosphere.

By attaching a protractor and a pitot tube together, an instrument was devised that was sensitive to direction as well as to the magnitude of velocity. As mentioned previously, this instrument was inserted through the cap into the vortex chamber. The recordings from the instrument were used to determine the circulation imparted to the flow.

The outputs from the pressure taps on the divergent tube and from the pitot tube were connected to a pressure transducer. The pressures were recorded with a Sanborn amplifier-recorder assembly. The transducer-amplifier-recorder combination produced results accurate to within $\pm .01$

inches of water, as determined by calibration tests.

Flow visualization was obtained by injecting smoke through the hole at the center of the vortex chamber cap. Smoke was produced from the reaction of titanium tetrachloride with the moisture in the air.

The air for the experiment was supplied by two large storage tanks. The air was passed through several pressure regulators and then through a calibrated rotameter. The flow rates used in this experiment varied from approximately 2.0 to 20.0 standard cubic feet per minute (scfm).

A plenum chamber received the air from the rotameter, and distributed it through six equally spaced and equal length hoses to the vortex chamber. The flow then passed through both the foam rubber and the vane section. At the vane section the flow attained a swirl. The resulting flow departed the vortex chamber, swirled through the divergent tube and finally exhausted into the atmosphere.

The following procedure was used in taking pressure readings from the divergent tube.

1. The vanes were set at one of the four desired angles;
2. The desired flow rate was set on the rotameter;
3. The transducer leads were attached to one pressure tap at a time;
4. A different flow rate was set on the rotameter and step (3) repeated; and
5. The vanes were set at a different angle and steps (2), (3), and (4) repeated.

The following procedure was used in obtaining data from the pitot tube:

6. Steps (1) and (2) were repeated;
7. The pitot tube was rotated slowly until a maximum pressure reading was recorded. At the point of maximum pressure, the direction of the maximum velocity was read from the protractor;
8. A new flow rate was set on the rotameter and step (7) repeated; finally
9. The vanes were set at a different angle and steps (2), (7), and (8) were repeated.

The data obtained in the manner described above were normalized through the use of appropriate reference values and presented graphically as will be discussed later.

3. Theoretical Considerations.

Lambourne and Bryer (3) suggested that the breakdown of a leading-edge vortex is associated with the adverse longitudinal pressure gradient which occurs in the flow field above a delta wing. It is for this purpose that the behavior of a simple vortex in an adverse pressure gradient, resulting from the divergence of the vortex tube, will be examined. Specifically, we will consider a streamwise vortex system consisting of a rotational core embedded in an external irrotational flow and analyze the behavior of the core as the longitudinal component of velocity decreases along the length of the tube.

The vortex system is shown in Figure 6. C_1 and C_2 are two cross-sections along an axisymmetric vortex whose axis is OX, and AB is the edge of the core outside of which the flow is irrotational. The flow between C_1 and C_2 is assumed to be incompressible and inviscid. The longitudinal component of velocity U_1 is uniform across the core and in the external flow at C_1 . At the cross-section C_2 , the external flow has a uniform longitudinal velocity component U_2 .

Considering an axisymmetric stream surface MN within the core which has radii r_1 and r_2 at C_1 and C_2 , and denoting u_2 and v_2 as the longitudinal and rotational components of velocity at the radial distance r_2 , expressions for u_2 and v_2 may be obtained in terms of V , U_1 , and U_2 as follows:

Equating the total pressures at C_1 and C_2 for a streamline on the stream surface MN through the use of the equation of Bernoulli, we have,

$$P_2 - P_1 = \frac{1}{2} \rho (U_1^2 + V_1^2 - u_2^2 - v_2^2) \quad (1)$$

where P_1 and P_2 are the static pressures at C_1 and C_2 respectively.

The condition of radial equilibrium at C_1 and C_2 may be expressed as

$$\frac{dP_1}{d\eta_1} = \frac{\rho V_1^2}{\eta_1} \quad \text{and} \quad \frac{dP_2}{d\eta_2} = \frac{\rho V_2^2}{\eta_2} \quad (2)$$

The conservation of angular momentum and mass flow rate yield respectively,

$$V_1 \eta_1 = V_2 \eta_2 \quad (3)$$

and

$$\frac{d\eta_1}{d\eta_2} = \frac{u_2 \eta_2}{U_1 \eta_1} \quad (4)$$

Differentiating equation (1) with respect to η_2 and using equations (2) to eliminate P_1 and P_2 , we have

$$\eta_2 \frac{du_2}{d\eta_2} + 2 \frac{V^2}{R_1^2 U_1} (\eta_1^2 - \eta_2^2) = 0 \quad (5)$$

Differentiating equation (5) with respect to η_2 and using equation (4), yields

$$\frac{d^2 u_2}{d\eta_2^2} + \frac{1}{\eta_2} \frac{du_2}{d\eta_2} + 4 \left(\frac{V}{U_1} \right)^2 \frac{1}{R_1^2} (u_2 - U_1) = 0 \quad (6)$$

Equation (6) may be normalized by writing

$$\eta = \frac{\eta_2}{R_2}, \quad u = \frac{u_2}{U_2}, \quad \alpha = 2 \frac{VR_2}{U_1 R_1}, \quad \beta = \frac{U_1}{U_2}$$

as

$$\frac{d^2 u}{d\eta^2} + \frac{1}{\eta} \frac{du}{d\eta} + \alpha^2 (u - \beta) = 0 \quad (7)$$

which is the zero-order Bessel equation.

Using the boundary condition that at $\eta = 1$, $u = 1$, and that the solutions in which $u \rightarrow \infty$ when $\eta = 0$ are not admitted, for obvious reasons, one has the general solution of the equation (7) as

$$u = \frac{1-\beta}{J_0(\alpha)} J_0(\alpha \eta) + \beta \quad (8)$$

Equation (8) gives the required distribution of longitudinal velocity component provided that β and α are specified. The parameter α may now be determined in terms of β and V/U_1 by considering the fact that the mass flow within the core at C_1 must equal the net mass flow across C_2 for the region $\eta_2 \leq R_2$.

Writing

$$R_1^2 U_1 = 2 R_2^2 U_2 \int_0^1 u \eta d\eta \quad (9)$$

and substituting u from equation (8), yields

$$\left(\frac{R_1}{R_2}\right)^2 = \frac{2(1-\beta)}{\beta J_0(\alpha)} \int_0^1 \eta J_0(\alpha \eta) d\eta + 1 \quad (10)$$

Upon performing the indicated integration, one has

$$\frac{V}{U_1} = \alpha \left(\frac{1}{4} - \frac{\beta-1}{2\beta\alpha} \frac{J_1(\alpha)}{J_0(\alpha)} \right)^{1/2} \quad (11)$$

The condition for the vortex breakdown through incipient stagnation at the axis is given by $u = 0$ at $\eta = 0$, which gives from equation (8)

$$\beta J_0(\alpha) = \beta - 1 \quad (12)$$

Inserting equation (12) into equation (11), we have the critical breakdown condition between V/U_1 and α as,

$$\frac{V}{U_1} = \alpha \left(\frac{1}{4} - \frac{1}{2\alpha} J_1(\alpha) \right)^{1/2} \quad (13)$$

The parameter V/U_1 is plotted as a function of $\beta = U_1/U_2$, through the use of equations (12) and (13), in Figure 7. The significance of this curve and its relations to the experimental data will be taken up in the next section.

4. Discussion of Theoretical and Experimental Results.

The static pressure distributions along the vortex tube for vane settings of 36.5° , 45° , 60° , and 70° are shown in Figures 8 through 11 in terms of the normalized pressure coefficient C_p and the dimensionless axial position x/r_1 for various rates of total flow. A critical examination of these figures yield the following obvious conclusions: (1) The data for a given vane setting shows a certain amount of scatter. This is not unexpected in view of the fact that one is dealing with rather small pressure changes. Furthermore, the effect of the boundary layers developing along the curved walls of the vortex chamber is not and cannot be expected to be proportional to the flow rate as far as the circulation retained at the entrance to the vortex tube is concerned; (2) The vortex breakdown is confined to a region extending from $x/r_1 = 3$ to 9. Considering the fact that the divergence of the tube starts at $x/r_1 = 4$, the effect of the divergence of the tube or in other words the significance of the adverse pressure gradient on the occurrence and location of the breakdown becomes apparent; finally, (3) it is observed that the breakdown is accompanied by stationary waves of finite amplitude. Although the existence of such waves has been theoretically predicted by Benjamin (9), no one, surprisingly enough, has experimentally verified their existence. To be sure, various attempts were made through the visualization of the vortex core to show that such waves arose from the vortex breakdown. But the difficulties encountered in the flow visualization techniques permitted only the observation of the rudiments of a wave train and the flow visualization agents introduced into the flow disintegrated rapidly. The examples of such flow visualization attempts made in the present study are shown in Figures 12 through 16. It is

possible to distinguish the first few of these waves prior to the rapid disintegration of the smoke. Despite the partial success of the photographic demonstration of the stationary waves, it is nevertheless clear from the pressure distribution curves that wavy flows do arise from the vortex breakdown. There appears reason enough to suppose that a periodic solution of the finite-perturbation equations comes closest, within the limitations of the ideal-fluid theory, to representing the observed situation. This interpretation is the same in principle as the one that was made by Benjamin as cited earlier.

The analysis presented in this thesis was not directed to the prediction of waves arising from the breakdown, but rather to the prediction of the incipient breakdown prior to the occurrence of waves which follow the breakdown.

Figure 7 shows that no curve for $\beta > 1.0$ intercepts the horizontal line corresponding to $V/U_1 = 1.2$, so that for this vortex no solution can be obtained however small the imposed retardation. This suggests that the vortex core (one for which $V/U_1 = 1.2$) is inherently unstable, and that some change, as yet unspecified, must occur spontaneously. It is relevant to remark that Squire (5) and Benjamin (9) using different approaches reached the conclusion that, for the same vortex model, $V/U_1 = 1.2$ (approximately) is the maximum critical value for the vortex breakdown.

Also shown in Figure 7 are the V/U_1 values calculated at the location of the first breakdown using the tangential velocities and circulations¹ determined with the pitot tube. It is apparent that all of the data for

¹The data are tabulated in Tables 1 through 4. $U_1 = Q / \pi r_1^2$
 $V = \Gamma / 2 \pi r_1$

all vane settings and flow rates fall within the region of expected breakdown below the theoretical curve.

In summary, it is noted that for any particular pair of values of V/U_1 and β there are a number of resulting flows each of which satisfies the specified conditions. The relation between these flow solutions and the original flow appears to be similar to the relation between the conjugate flows discussed by Benjamin. For the particular condition of imposed retardation or adverse pressure gradients examined numerically, there is a critical relation between V/U_1 and β for which physically realistic flow solutions can just occur.

As to the formation of waves arising from the breakdown, it is clear that the state of flow upstream from the breakdown point is supercritical, i.e., stationary waves of finite amplitude cannot be formed upon it by any non-dissipative process. Downstream from the breakdown point, however, the state of flow is subcritical, so that stationary periodic waves can arise upon it. The subcritical flow, in comparison with the supercritical flow, has the greater value of flow force just as in the case of a hydraulic jump. Thus, a flow formed by the superposition of stationary waves may exist from the breakdown point since the flow-force balance needed for a steady state is achieved by the effect of wave resistance. In other words, the excess flow force is absorbed by wave formation; or alternatively, if the original flow is a strong supercritical flow and consequently the flow-force difference is large, such a violent wave-making action is induced that the leading wave breaks in the form of a burst of turbulence as photographed in Figures 12 through 16.

5. Conclusions.

1. Vortex breakdown is followed by a series of standing waves. The presence of these waves is demonstratable through the study of the longitudinal pressure distribution. The observations of a filament of smoke or dyed fluid shows that a filament originally along the axis goes into a spiralling motion after a breakdown and eventually breaks into a random turbulent motion.

2. Theoretical calculations on the effect of imposing an adverse pressure gradient, or longitudinal retardation, on an inviscid model-vortex show that it is possible for such a change to lead to breakdown and to an inner core of reversed flow. The most significant theoretical observation is that an imposed change beyond a critical value can lead to a drastic change of flow structure.

3. The vortex core for which $V/U_1 = 1.2$, is inherently unstable. This value is in agreement with those predicted by Squire and Benjamin using different approaches for the same vortex model. The experimentally predicted parameters (V/U_1 , β) regarding the occurrence of breakdown are in good agreement with those predicted theoretically.

4. The theoretical and experimental work described herein show that for a given upstream and downstream conditions, there are two different states of flow through the vortex tube. The location of the breakdown is determined by the conditions prevailing in the downstream section of the tube, in the same way that location of a hydraulic jump on a supercritical stream in an open channel is determined by the back water conditions. Moreover, just as some sort of obstruction in the channel is necessary to precipitate a hydraulic jump on a supercritical stream, the vortex breakdown requires one or more triggering agencies such as the adverse pressure gradient created by the divergence of the vortex tube.

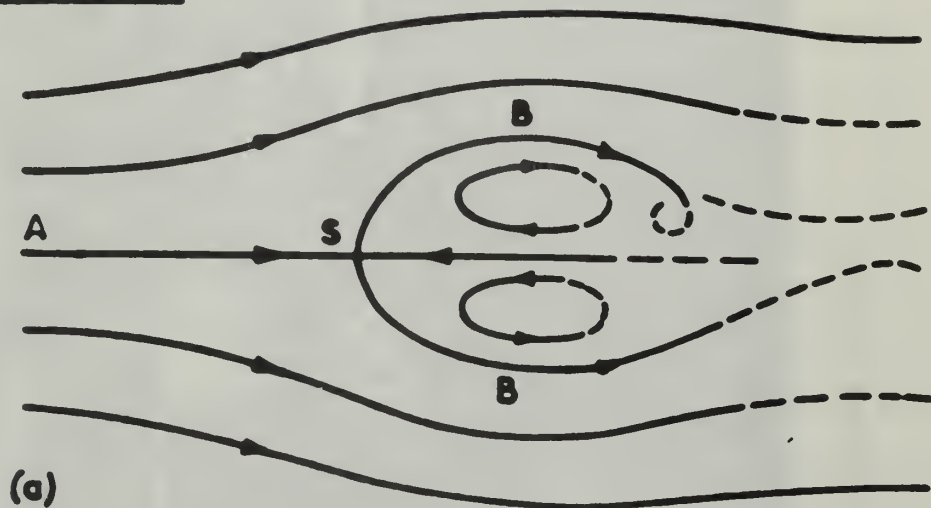
6. Recommendations for Future Work.

1. Change the length and the angle of divergence of the vortex tube to cover other ranges of the flow parameters.
2. Repeat all of the experiments using water as the working fluid.
3. Obtain velocity profiles at various sections of the vortex for the purpose of carrying out a theoretical analysis through the use of the Navier-Stokes equations and for the purpose of demonstrating the existence of secondary swirling flows within the waves following the breakdown.
4. Compute the development of the swirling flow in the downstream direction by a finite-difference technique, with the shape of the tube and the initial, upstream, conditions prescribed in order to determine if the occurrence of a singularity in the mathematical solution is related to the pronounced deceleration of the axial flow prior to breakdown.

BIBLIOGRAPHY

1. Vonnegut, B., "A Vortex Whistle," Journal of the Acoustical Society of America, Vol. 26, 1954, p. 18.
2. Smith, J. L., "An Analysis of the Vortex Flow in Cyclone Separator," Journal of Basic Engineering, Trans. ASME, Series D, Vol. 84, 1962, p. 609.
3. Lambourne, N. C., and Bryer, D. W., "The Bursting of Leading Edge Vortices - Some Observations and Discussion of the Phenomenon," Aeronautical Research Council, U. K., R & M-3282, April, 1962, pp. 36.
4. Peckham, D. H., "Preliminary Results of Low Speed Wind Tunnel Tests on a Gothic Wing of Aspect Ratio 1.0." RAE Technical Note Aero No. 2504, 1957.
5. Squire, H. G., "Analysis of the Vortex Breakdown Phenomenon, Part-1," Aero Dept., Imperial College, Report No. 102, 1960, ARC 21977.
6. Harvey, J. K., "Some Observations of the Vortex Breakdown Phenomenon," Journal of Fluid Mechanics, Vol. 14, December 1962, p. 585.
7. Chanaud, R. C., "Observations of Oscillatory Motion in Certain Swirling Flows," Journal of Fluid Mechanics, Vol. 21, January, 1965, pp. 111-127.
8. Gartshore, I. S., "Recent Work in Swirling Incompressible Flow," National Research Council, Canada, Aeronautical Report LR-343, 1962.
9. Benjamin, T. B., "Theory of the Vortex Breakdown Phenomenon," Journal of Fluid Mechanics, Vol. 14, December, 1962, pp. 593-629.
10. Benjamin, T. B., "Significance of the Vortex Breakdown Phenomenon," Journal of Basic Engineering, Trans. ASME, Series D, Vol. 87, June, 1965, pp. 518-524.
11. Hall, M. G., "A Numerical Investigation of Vortex Breakdown," Royal Aircraft Establishment, U. K., Tech. Memo Aero 926, March, 1966, pp. 17.
12. Sarpkaya, T., "Forced and Periodic Vortex Breakdown," Journal of Basic Engineering, Trans. ASME, Series D, Vol. 89, No. 3, September, 1967, pp. 609-616.

Axlsymmetric form



Spiral form

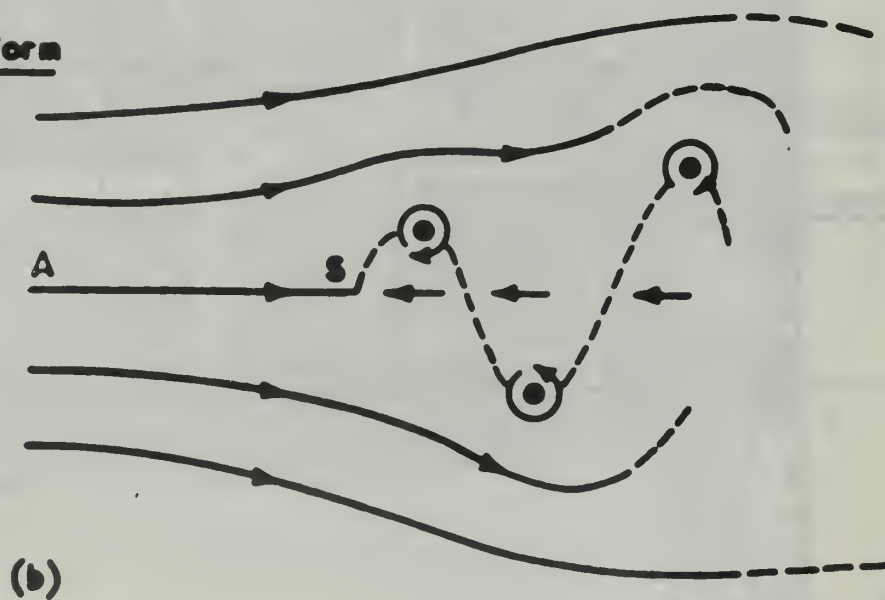


Fig. 1 THE TWO FORMS OF VORTEX BREAKDOWN

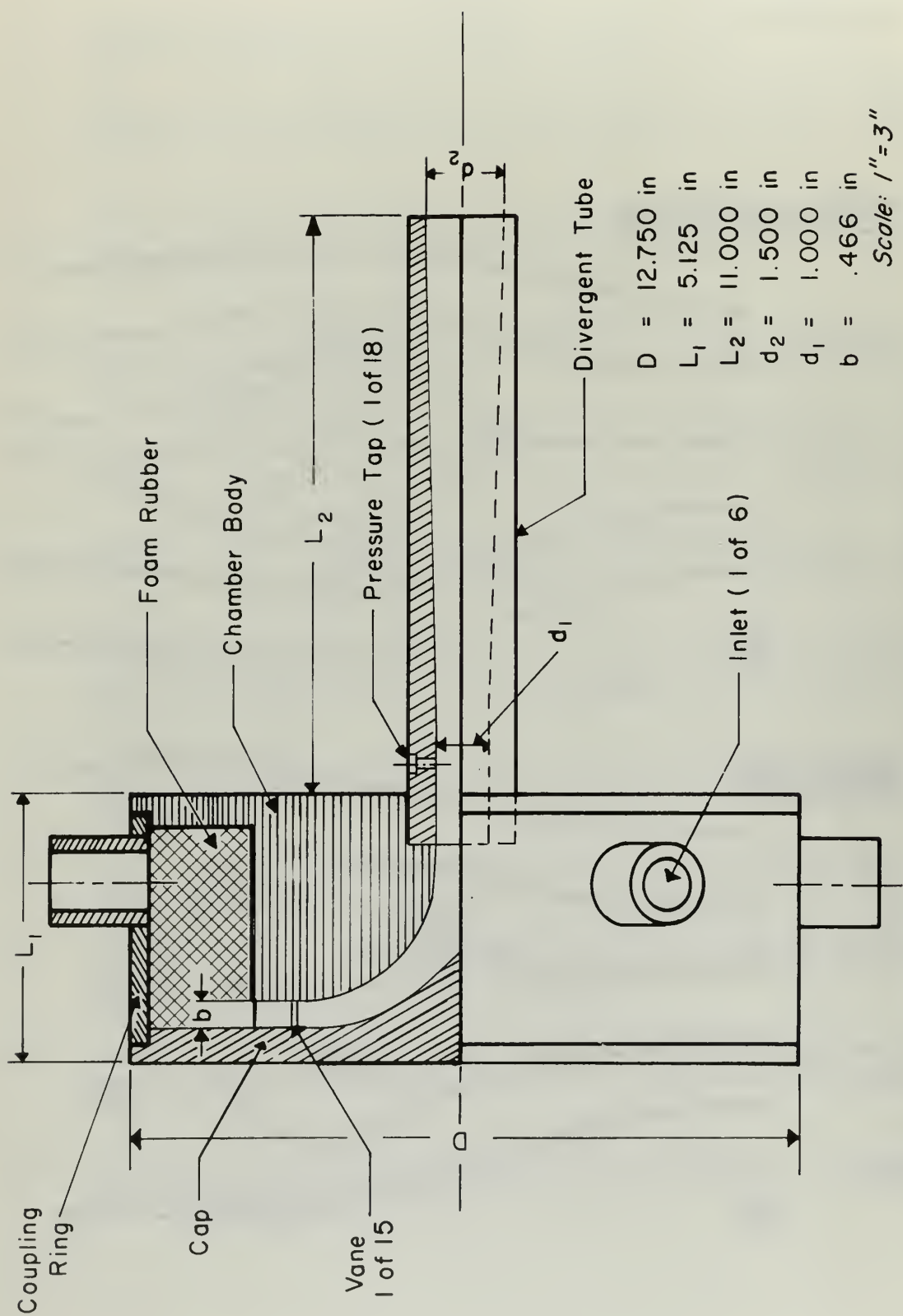


Fig. -2- SCHEMATIC OF VORTEX CHAMBER AND DIVERGENT TUBE

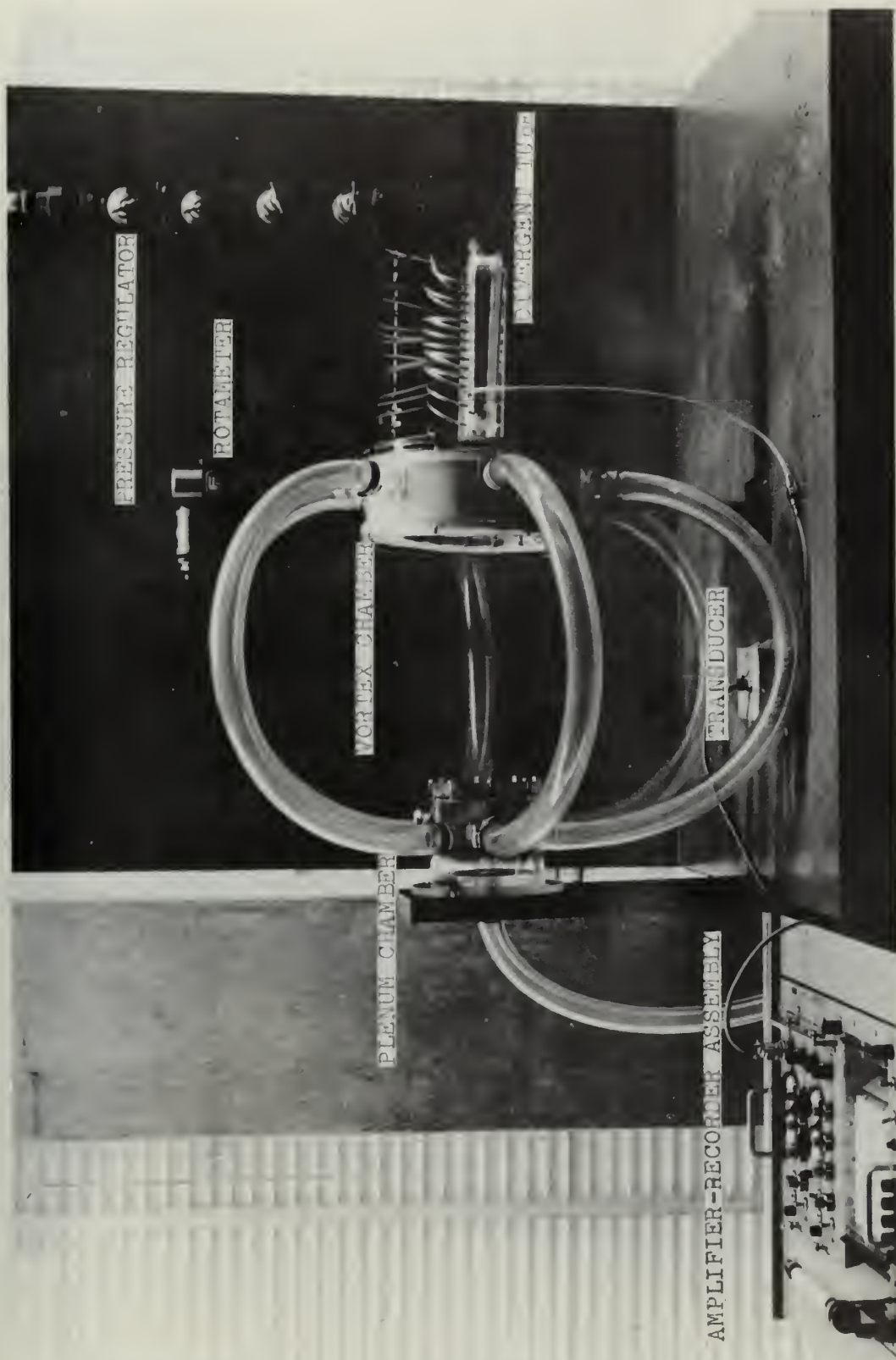


Fig. 3 ARRANGEMENT OF EXPERIMENTAL APPARATUS

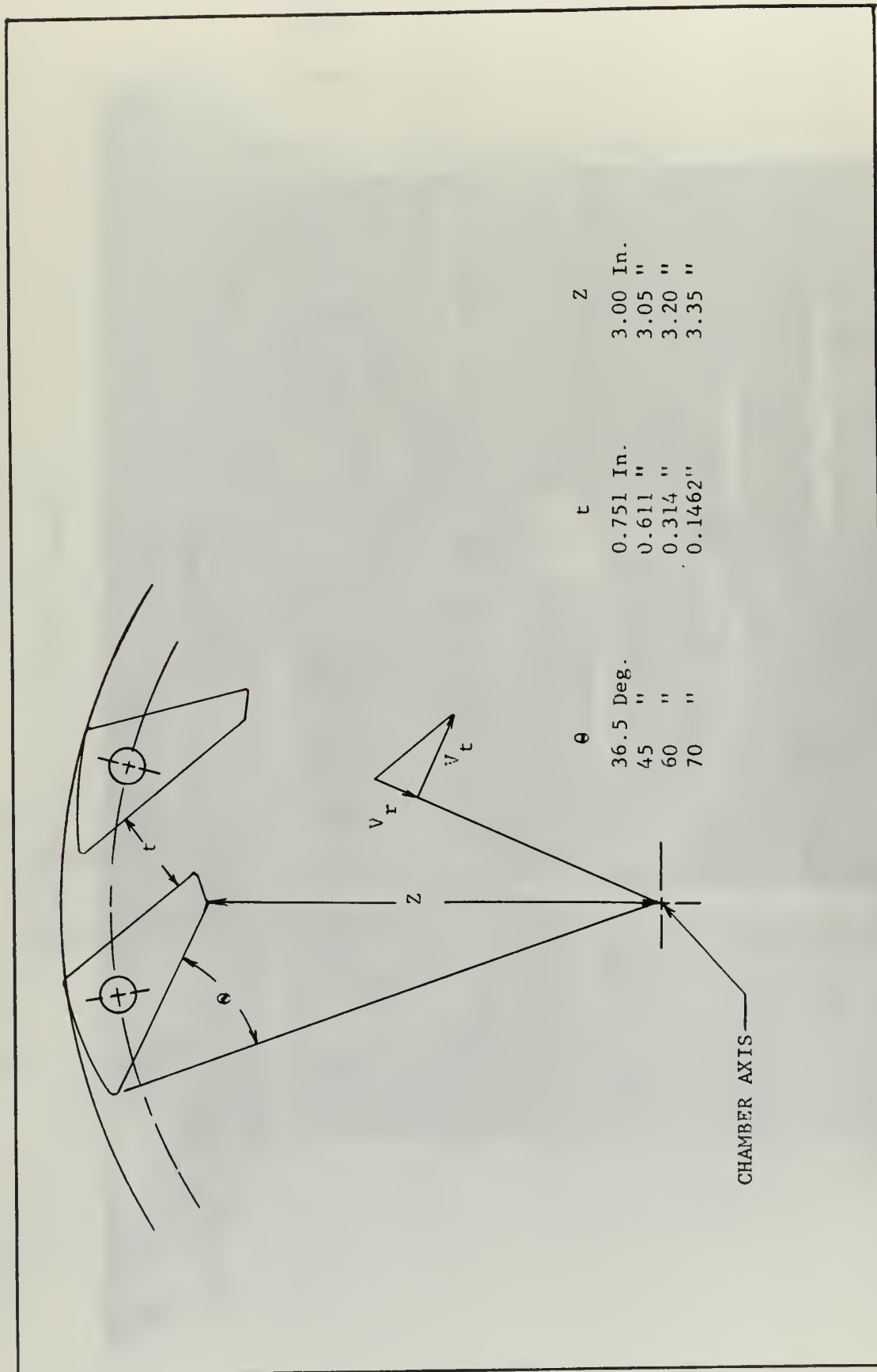


Fig. 4 SKETCH OF VANE ORIENTATION

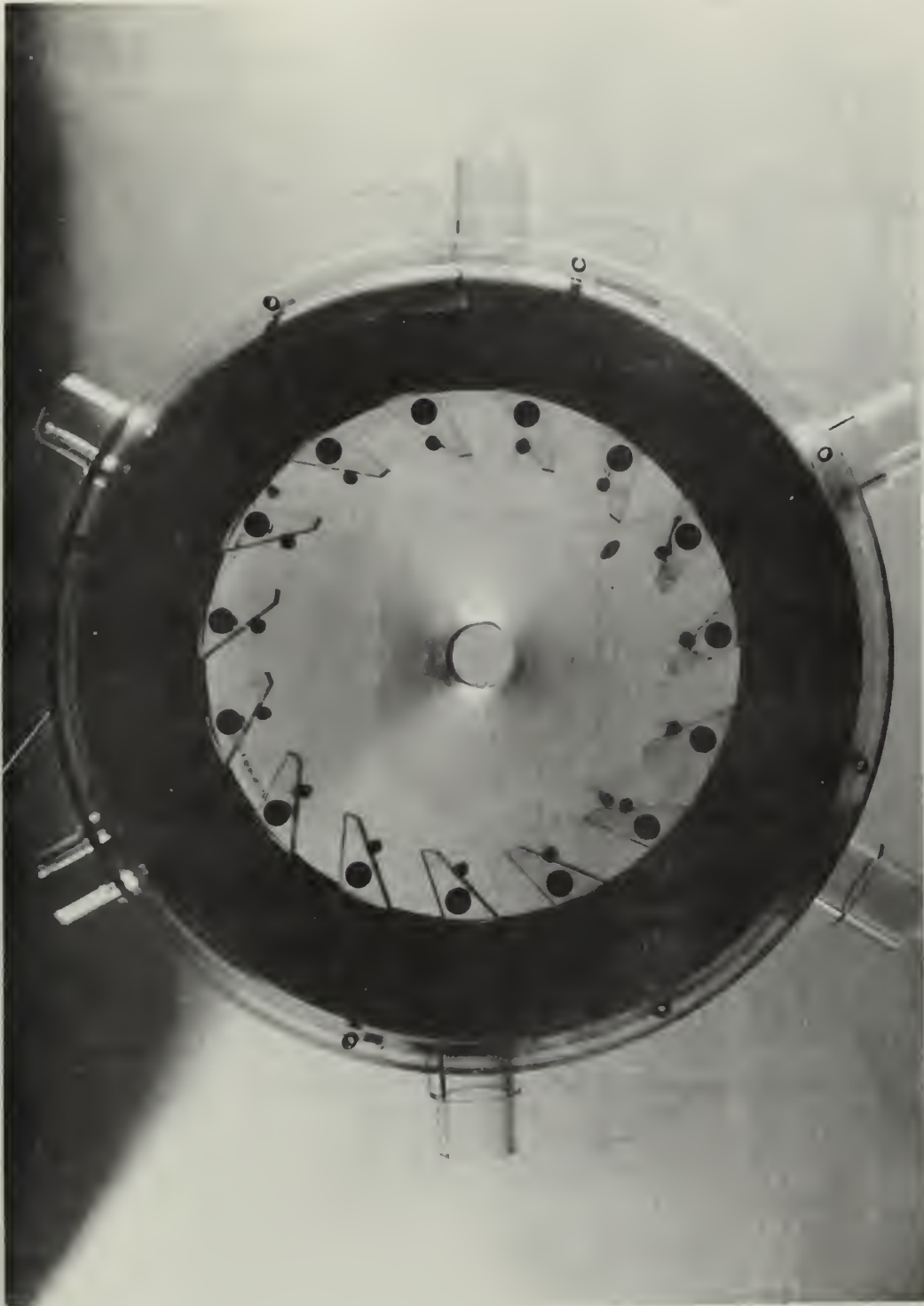


Fig. 5 PHOTOGRAPH OF VANE SECTION AND CHAMBER INLETS

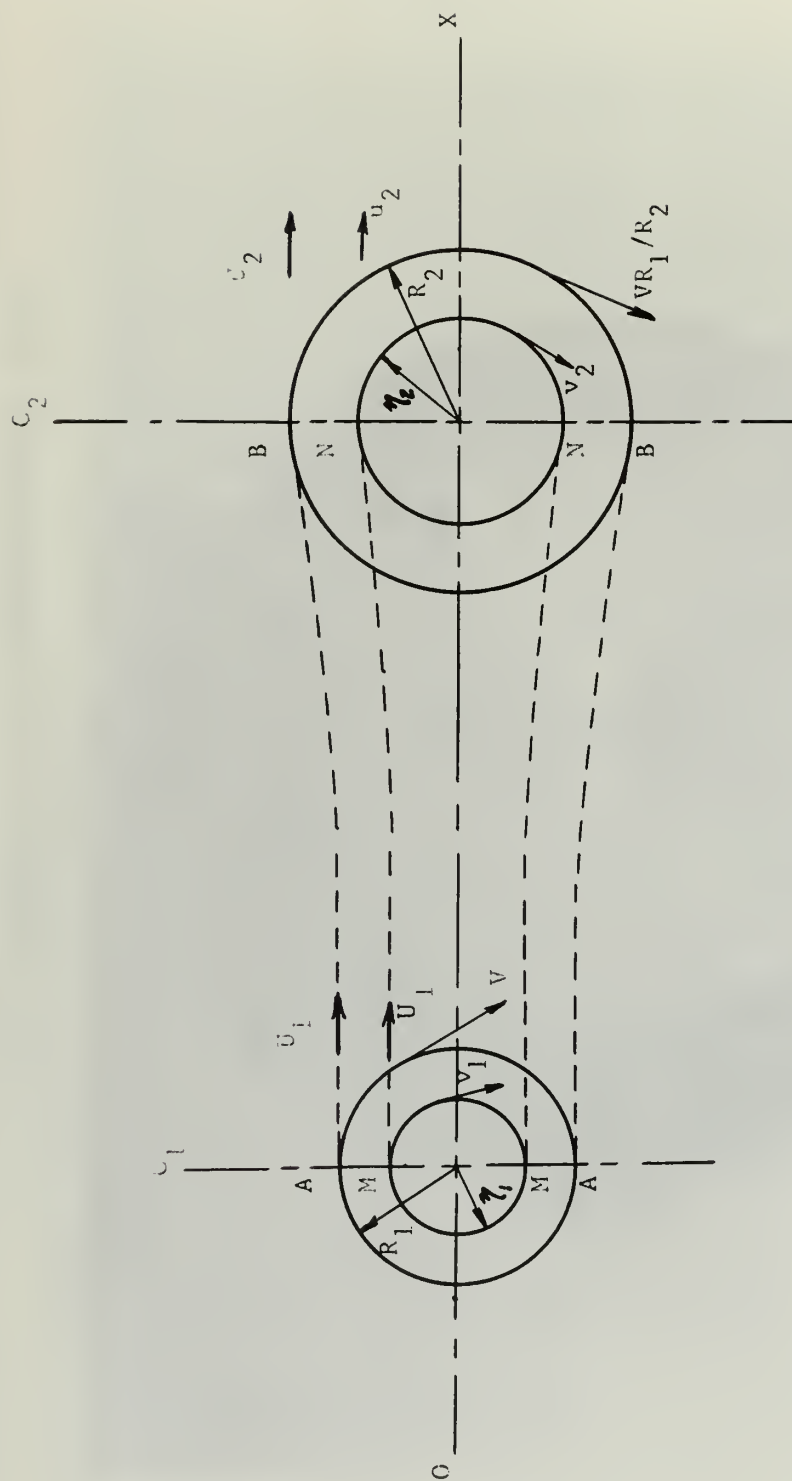


Fig. 6 MATHEMATICAL MODEL OF THE VORTEX CORE

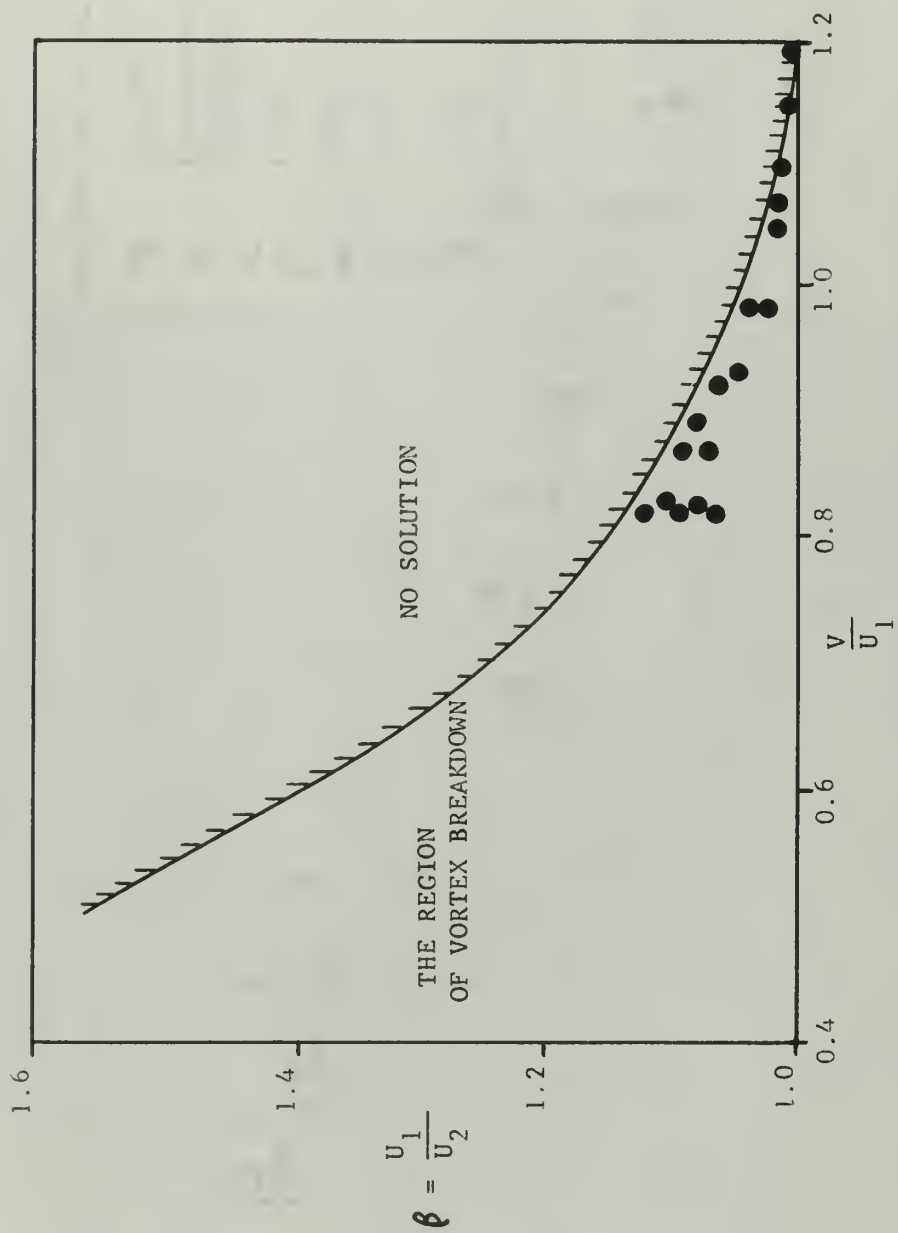


Fig. 7 NORMALIZED AXIAL VELOCITY VS. TANGENTIAL VELOCITY
(THE PREDICTION OF THE REGION OF VORTEX BREAKDOWN)

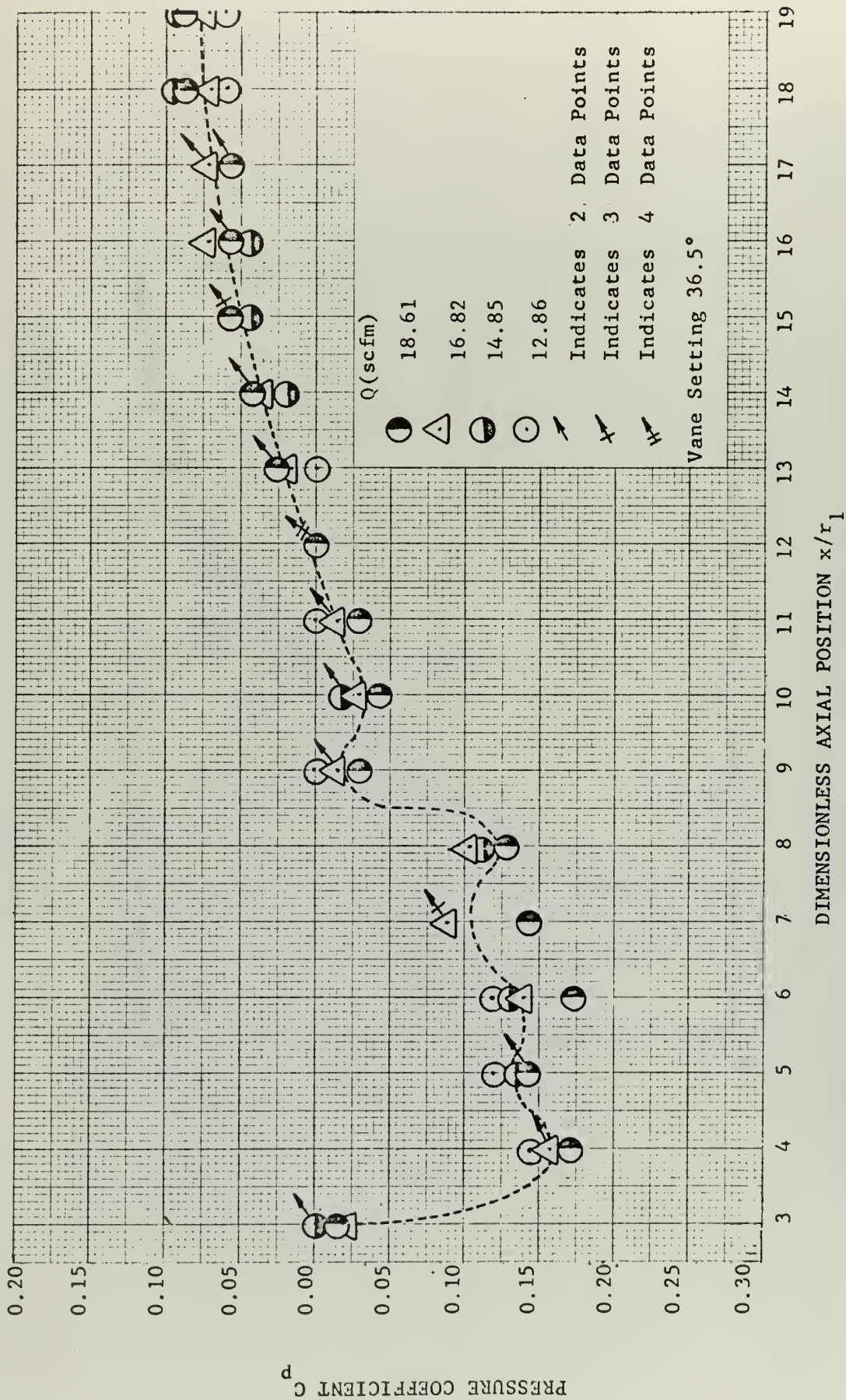


Fig. 8 STATIC PRESSURE DISTRIBUTION ALONG TUBE (VANE SETTING 36.5 deg.)

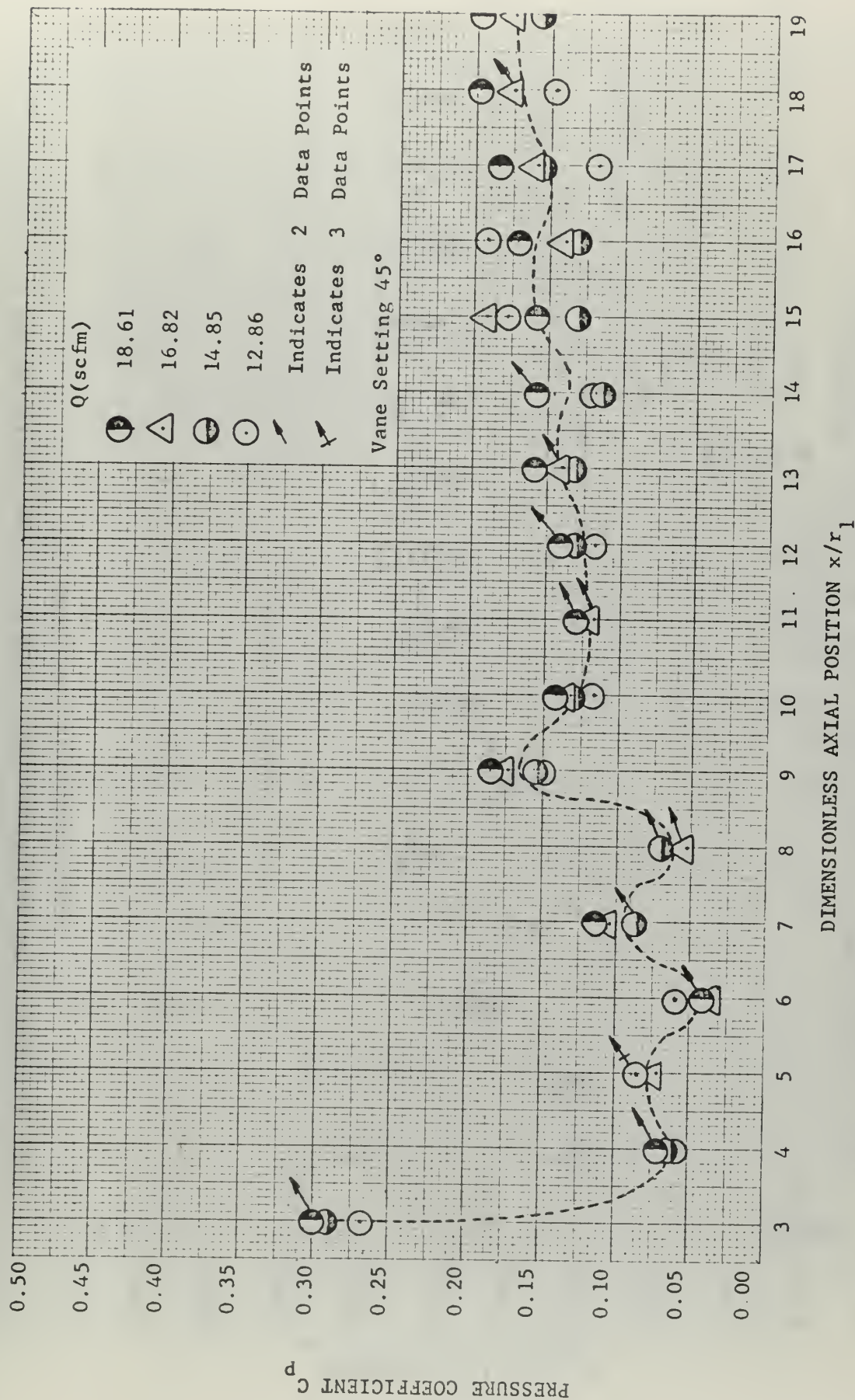


Fig. 9 STATIC PRESSURE DISTRIBUTION ALONG TUBE (VANE SETTING 45 Deg.)

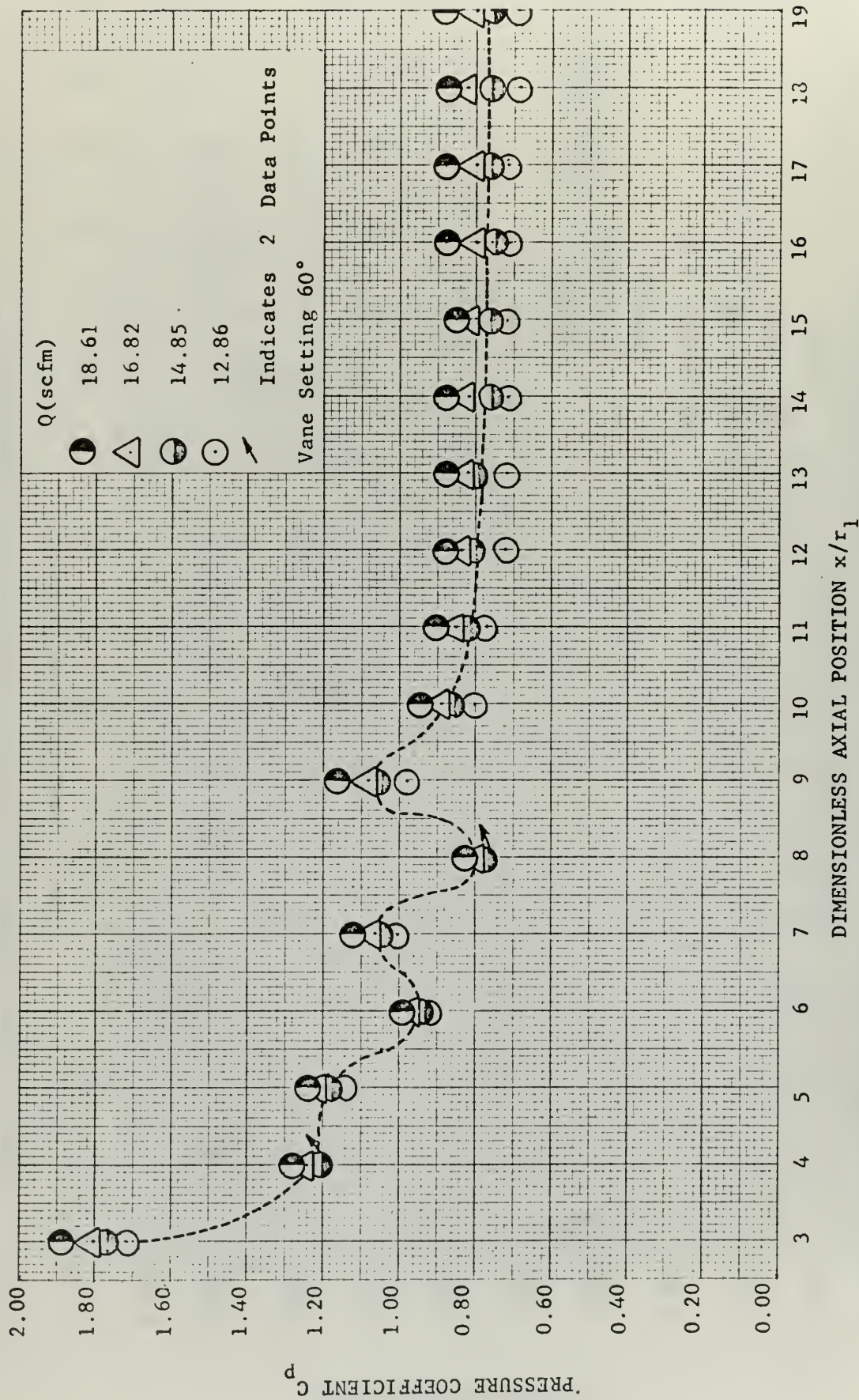


Fig. 10 STATIC PRESSURE DISTRIBUTION ALONG TUBE (VANE SETTING 60 Deg.)

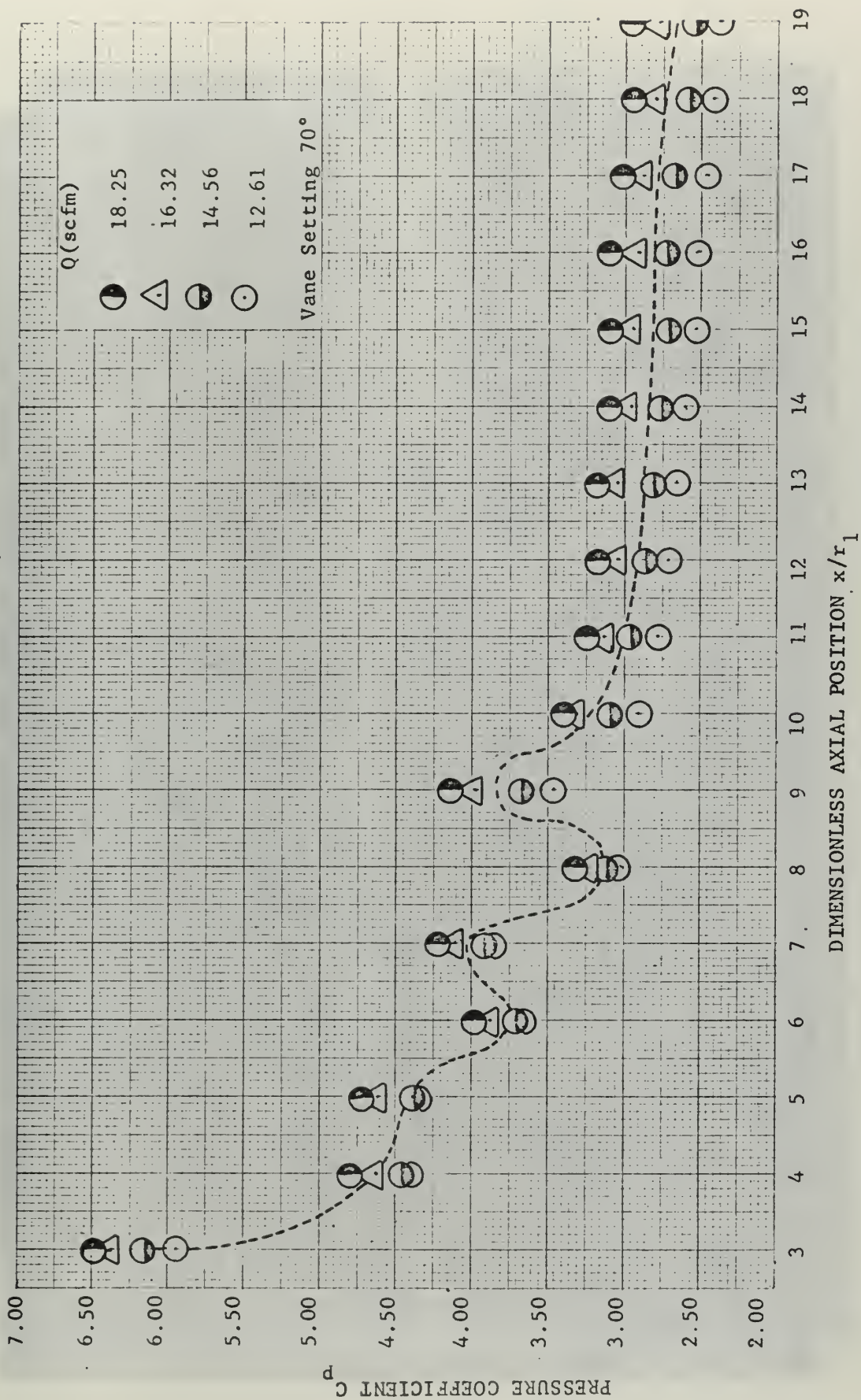


Fig. 11 STATIC PRESSURE DISTRIBUTION ALONG TUBE (VANE SETTING 70° Deg.)



Fig. 12 EXAMPLE OF VISUALIZATION OF VORTEX BREAKDOWN



Fig. 13 EXAMPLE OF VISUALIZATION OF VORTEX BREAKDOWN



Fig. 14 EXAMPLE OF VISUALIZATION OF VORTEX BREAKDOWN



Fig. 15 EXAMPLE OF VISUALIZATION OF VORTEX BREAKDOWN



Fig. 16 EXAMPLE OF VISUALIZATION OF VORTEX BREAKDOWN

TABLE - 1 EXPERIMENTAL DATA FOR THE CALCULATION OF CIRCULATION FOR THE VANE SETTING OF 36.5 Deg.

Flow Rate $Q(\text{Ft}^3/\text{Min})$	Total Velocity $V'(\text{Ft}/\text{Sec})$	Probe Angle $\gamma(\text{Deg})$	Tangential Velocity $V_t(\text{Ft}/\text{Sec})$	Circulation $\Gamma(\text{Ft}^2/\text{Sec})$
18.80	37.8	137	37.2	13.65
16.82	31.4	135	30.7	11.80
14.85	27.1	137	26.6	9.76
12.89	23.2	132	27.4	9.12
10.90	20.1	132	19.40	7.90
8.92	17.70	130	17.01	7.16
6.94	13.38	130	12.89	5.43

TABLE - 2 EXPERIMENTAL DATA FOR THE CALCULATION OF CIRCULATION FOR THE VANE SETTING OF 45 Deg.

Flow Rate $Q(\text{Ft}^3/\text{Min})$	Total Velocity $V'(\text{Ft}/\text{Sec})$	Probe Angle $\gamma(\text{Deg})$	Tangential Velocity $V_t(\text{Ft}/\text{Sec})$	Circulation $\Gamma(\text{Ft}^2/\text{Sec})$
18.61	40.2	138	39.6	14.30
16.82	35.4	138	34.8	12.55
14.85	31.4	138	30.9	11.12
12.86	26.8	136	26.3	9.90
10.90	23.1	136	22.7	8.54
8.90	18.90	130	18.15	7.65
6.93	15.00	130	14.41	6.09

TABLE - 3 EXPERIMENTAL DATA FOR THE CALCULATION OF CIRCULATION FOR THE VANE SETTING OF 60 Deg.

Flow Rate Q(Ft ³ /Min)	Total Velocity V'(Ft/Sec)	Probe Angle γ (Deg)	Tangential Velocity V _t (Ft/Sec)	Circulation Γ (Ft ² /Sec)
18.61	108.0	138	106.2	38.3
16.82	94.5	138	93.0	33.5
14.85	83.2	138	81.9	29.5
12.86	70.0	138	68.9	24.5
10.90	59.7	138	58.7	21.2
8.90	46.2	138	45.5	16.40
6.93	35.4	138	34.8	12.75
4.95	25.0	138	24.6	8.86

TABLE - 4 EXPERIMENTAL DATA FOR THE CALCULATION OF CIRCULATION FOR THE VANE SETTING OF 70 Deg.

Flow Rate Q(Ft ³ /Min)	Total Velocity V'(Ft/Sec)	Probe Angle γ (Deg)	Tangential Velocity V _t (Ft/Sec)	Circulation Γ (Ft ² /Sec)
18.61	177.0	138	174.5	62.8
16.82	155.0	138	152.9	55.9
14.85	135.8	138	133.9	48.6
12.86	116.0	135	113.0	44.5
10.90	97.0	135	94.5	37.2
8.90	77.7	135	75.6	29.8
6.93	57.9	133	56.3	23.1
4.95	39.5	135	38.5	15.20

INITIAL DISTRIBUTION LIST

	No. Copies
1. Defense Documentation Center Cameron Station Alexandria, Virginia 22314	20
2. Library Naval Postgraduate School Monterey, Calif.	2
3. Naval Ship Systems Command (Code 2052) Navy Department Washington, D. C. 20360	1
4. Mechanical Engineering Department Naval Postgraduate School Monterey, Calif.	2
5. Professor T. Sarpkaya Chairman, Mechanical Engineering Department Naval Postgraduate School Monterey, Calif.	5
6. LT J. R. Fantin, USN Ship Repair Facility Yokosuka, Japan FPO San Francisco 96662	2

DOCUMENT CONTROL DATA - R & D

Security classification of title, body of abstract and indexing annotation must be entered when the overall report is classified)

1. ORIGINATING ACTIVITY (Corporate author) Naval Postgraduate School, Monterey, Calif.		2a. REPORT SECURITY CLASSIFICATION Unclassified	
		2b. GROUP	
3. REPORT TITLE An Investigation of the Characteristics of Swirling Flow in a Diverging Tube			
4. DESCRIPTIVE NOTES (Type of report and, inclusive dates) None			
5. AUTHOR(S) (First name, middle initial, last name) Fantin, Jon Ronald			
6. REPORT DATE June 1968		7a. TOTAL NO. OF PAGES 47	7b. NO. OF REFS 12
8a. CONTRACT OR GRANT NO.		9a. ORIGINATOR'S REPORT NUMBER(S) N/A	
9. PROJECT NO. N/A			
c.		9b. OTHER REPORT NO(S) (Any other numbers that may be assigned this report)	
d.			
10. DISTRIBUTION STATEMENT [REDACTED]			
11. SUPPLEMENTARY NOTES		12. SPONSORING MILITARY ACTIVITY U. S. Army	
13. ABSTRACT <p>The effect of an imposed pressure gradient on the core of a vortex is examined both theoretically and experimentally. The test apparatus consisted of a vortex chamber and a diverging tube. The swirling flow was generated by means of adjustable vanes at the periphery of the vortex chamber and by introducing varying amounts of air. Pressure distributions were obtained along the wall of the tube for various flows and vane settings. In addition, the core of the vortex was photographed by introducing smoke at the axis of the vortex chamber.</p> <p>The theoretical and experimental results show the existence of standing waves arising from the vortex breakdown and the existence of critical conditions, depending on the ratio of the rotational and longitudinal velocity components, beyond which drastic changes of flow structure must occur. The theoretical results were found to be closely related to the observed phenomena.</p>			

14

KEY WORDS

LINK A

LINK B

LINK C

ROLE

WT

ROLE

WT

ROLE

WT

Vortex Breakdown

Swirling Flow in a Divergent Tube

1

thesF223

A -

DUDLEY KNOX LIBRARY



3 2768 00407350 2

DUDLEY KNOX LIBRARY